frontiers in Oncology

ORIGINAL RESEARCH
published: 25 April 2019
doi: 10.3389/fonc.2019.00313

Glesatinib, a c-MET/SMO Dual Inhibitor, Antagonizes P-glycoprotein Mediated Multidrug Resistance in Cancer Cells

*Qingbin Cui[1,2], Chao-Yun Cai[2], Hai-Ling Gao[2,3], Liang Ren[1], Ning Ji[2,4], Pranav Gupta[2], Yuqi Yang[2], Suneet Shukla[5], Suresh V. Ambudkar[5], Dong-Hua Yang[2] and Zhe-Sheng Chen[2]**

[1] School of Public Health, Guangzhou Medical University, Guangdong, China, [2] Department of Pharmaceutical Sciences, College of Pharmacy and Health Sciences, St. John's University, Queens, NY, United States, [3] Department of Histology and Embryology, Clinical Medical College, Weifang Medical University, Weifang, China, [4] Tianjin Key Laboratory on Technologies Enabling Development of Clinical Therapeutics and Diagnostics, School of Pharmacy, Tianjin Medical University, Tianjin, China, [5] Laboratory of Cell Biology, Center for Cancer Research, National Cancer Institute, NIH, Bethesda, MD, United States

OPEN ACCESS

Edited by:
Massimo Broggini, Istituto Di Ricerche Farmacologiche Mario Negri, Italy

Reviewed by:
Fabrizio Martelli, Istituto Superiore di Sanità (ISS), Italy
Kamini Singh, Memorial Sloan Kettering Cancer Center, United States
Sandro Cosconati, Università degli Studi della Campania Luigi Vanvitelli Caserta, Italy

***Correspondence:**
Zhe-Sheng Chen
chenz@stjohns.edu

Specialty section:
This article was submitted to Cancer Molecular Targets and Therapeutics, a section of the journal Frontiers in Oncology

Received: *25 January 2019*
Accepted: *08 April 2019*
Published: *25 April 2019*

Citation:
Cui Q, Cai C-Y, Gao H-L, Ren L, Ji N, Gupta P, Yang Y, Shukla S, Ambudkar SV, Yang D-H and Chen Z-S (2019) Glesatinib, a c-MET/SMO Dual Inhibitor, Antagonizes P-glycoprotein Mediated Multidrug Resistance in Cancer Cells. Front. Oncol. 9:313. doi: 10.3389/fonc.2019.00313

Multidrug resistance (MDR) is one of the leading causes of treatment failure in cancer chemotherapy. One major mechanism of MDR is the overexpressing of ABC transporters, whose inhibitors hold promising potential in antagonizing MDR. Glesatinib is a dual inhibitor of c-Met and SMO that is under phase II clinical trial for non-small cell lung cancer. In this work, we report the reversal effects of glesatinib to P-glycoprotein (P-gp) mediated MDR. Glesatinib can sensitize paclitaxel, doxorubicin, colchicine resistance to P-gp overexpressing KB-C2, SW620/Ad300, and P-gp transfected Hek293/ABCB1 cells, while has no effect to their corresponding parental cells and negative control drug cisplatin. Glesatinib suppressed the efflux function of P-gp to [^{3}H]-paclitaxel and it didn't impact both the expression and cellular localization of P-gp based on Western blot and immunofluorescent analysis. Furthermore, glesatinib can stimulate ATPase in a dose-dependent manner. The docking study indicated that glesatinib interacted with human P-gp through several hydrogen bonds. Taken together, c-Met/SMO inhibitor glesatinib can antagonize P-gp mediated MDR by inhibiting its cell membrane transporting functions, suggesting new application in clinical trials.

Keywords: multidrug resistance, P-gp, glesatinib, reversal effects, mechanism

INTRODUCTION

Multidrug resistance (MDR) is the one of the major challenges in cancer treatment (1). MDR refers to a phenomenon that cancer cell once becomes resistant to one chemotherapeutic, accompanied by cross resistant to other chemotherapeutics that are structurally and mechanistically different (2). MDR is one of the major causes of failure in cancer treatment. The mechanisms of MDR involve dynamic ATP-binding cassette (ABC) transporters (3, 4), oncogenes mutations (5), microenvironment changes (6), reprogramed cancer cell metabolism (7, 8), efficient DNA repairing (9, 10), survived cancer stem cells (11, 12), and activated detoxifying systems (13, 14). Novel effective remedies are urgently needed to circumvent MDR.

ABC transporters are a group of active transporter proteins that have diverse functions and are present in the membrane of both prokaryotes and eukaryotes, acting as protecting enzymes against xenobiotic, including many chemotherapeutics (15, 16). One of the most well studied ABC transporters is P-glycoprotein (P-gp), which is encoded by ABCB1 genes. P-gp contributes in pumping out many different kinds of anticancer drugs, namely, taxanes, anthracyclines, vinca alkaloids, and epipodophyllotoxins (17–24). To counteract the negative regulation of chemotherapy by P-gp, three generations of inhibitors (both specific and non-specific) have been developed and some of them have been introduced into clinical trials (25). However, due to unexpected adverse effects or severely drug-drug interaction, none of them have been approved by FDA (3, 26). There is an unmet need for effective and safe reversal agents for clinical use. Recently, certain tyrosine kinase inhibitors (TKIs) have been found to exert MDR reversal effect via regulating P-gp at non-toxic concentration (27–31), suggesting new regimens in the treatment of resistant cancer. TKI glesatinib (**Figure 1A**), a c-MET/SMO dual inhibitor (32, 33), is now under Phase II clinical trials in combination with Nivolumab in treatment of the non-small cell lung cancer (NSCLC). More importantly, we found that glesatinib can antagonize P-gp mediated MDR. Here, we report the reversal effects of glesatinib and the underlying mechanisms.

MATERIALS AND METHODS

Chemicals

Glesatinib (99% purity as measured by high performance liquid chromatography) was purchased from ChemieTek (Indianapolis, IN). Dulbecco's modified Eagle's Medium (DMEM), bovine serum albumin (BSA), fetal bovine serum (FBS), penicillin/streptomycin and trypsin 0.25% were purchased from Hyclone (GE Healthcare Life Science, Pittsburgh, PA). The monoclonal antibodies for ABCB1 (C219) and GAPDH (MA5-15738), Alexa Fluor 488 conjugated goat anti-mouse IgG secondary antibody were purchased from Thermo Fisher Scientific Inc (Rockford, IL), dimethylsulfoxide (DMSO), 3-(4,5-dimethylthiazol-yl)-2,5-diphenyltetrazolium bromide (MTT), Triton X-100, 4',6-diamidino-2-phenylindole (DAPI), paraformaldehyde, paclitaxel, doxorubicin, colchicine, cisplatin, verapamil and Ko 143 were purchased from Sigma-Aldrich (St. Louis, MO). [^{3}H]-paclitaxel (15 Ci/mmol) was purchased from Moravek Biochemicals, Inc (Brea, CA). All other chemicals were purchased from Sigma Chemical Co (St. Louis, MO).

Cell Lines and Cell Culture

The human epidermoid carcinoma cell line KB-3-1 and its colchicine-selected P-gp-overexpressing KB-C2 cells, the human colon cancer cell line SW620 and its doxorubicin-selected P-gp-overexpressing SW620/Ad300 cells, the NSCLC cell line NCI-H460 and its mitoxantrone-selected ABCG2-overexpressing NCI-H460/MX20 cells, were used for P-gp and ABCG2 reversal study, respectively. The HEK293/pcDNA3.1, HEK293/ABCB1 cells lines were established by transfecting HEK293 cells with either the empty pcDNA3.1 vector or the vector containing full length ABCB1 (HEK293/ABCB1), and were cultured in a medium containing 2 mg/mL of G418. All cell were cultured at 37°C, using 5% CO_2 with DMEM containing 10% FBS and 1% penicillin/streptomycin. All drug resistant cell lines were grown as adherent monolayer in a drug-free culture media for more than 2 weeks prior to their use.

Cytotoxicity and Reversal Experiments

The cytotoxicity and reversal experiments of glesatinib to KB-3-1, KB-C2, SW620, SW620/Ad300, HEK293/pcDNA3.1, HEK293/ABCB1 cells were performed by using the MTT colorimetric assay (34). For reversal experiments, the applied concentrations of glesatinib were 1 and 3 μM according to the results of cytotoxicity experiments. All of the experiments were repeated at least three times, and the mean and standard deviation (SD) values were calculated. Verapamil (3 μM) was used as a positive control inhibitor of P-gp, Ko 143 was used as a positive control inhibitor of ABCG2, cisplatin, a non-P-gp substrate, was used as a negative control.

Western Blot Analysis

Dose-dependent (0, 0.3, 1, 3 μM) and time-dependent (0, 24, 48, 72 h) of glesatinib on the expression of P-gp were determined. Twenty microgram protein cell lysates were loaded in each lane. The presence of P-gp was determined using monoclonal antibody C219 (dilution 1:200). GAPDH was used to confirm equal loading in each lane in the samples prepared from cell lysates. The resulting protein bands were quantified by using Image J software. The detailed protocol of Western blot analysis was carried out as previously described (35).

Immunofluorescence Analysis

SW620, SW620/Ad300 cells were seeded (1×10^4/well) in 24-well plates and cultured at 37°C for 24 h, followed by incubation with 3 μM glesatinib for 0, 24, 48, and 72 h, respectively. Then cells were fixed in 4% paraformaldehyde for 5 min and permeabilized by 0.1% Triton X-100 for 5 min before blocked with 6% BSA for 1 h at 37°C. The presence of P-gp was determined using monoclonal antibody F4 (dilution 1:1000) for incubation at 4°C overnight. Alexa Fluor 488 conjugated secondary antibody (1:1000) was used for incubation at 37°C for 1 h. After washing with iced PBS, DAPI (1 μg/mL) was used to counterstain the nuclei. Immunofluorescence images were collected using an EVOS FL Auto fluorescence microscope (Life Technologies Corporation, Gaithersburg, MD).

ATPase Assay

The vanadate-sensitive ATPase activity of ABCB1 in membrane vesicles of High Five insect cells was measured as previously described (36). Briefly, the membrane vesicles (10 μg of protein) were incubated in ATPase assay buffer [composed by 50 mmol/L MES (pH 6.8), 50 mmol/L KCl, 5 mmol/L sodium azide, 2 mmol/L EGTA, 2 mmol/L DTT, 1 mmol/L ouabain, and 10 mmol/L $MgCl_2$] with or without 0.3 mmol/L vanadate at 37°C for 5 min, then were incubated with different concentrations (ranging from 0 to 40 μM) of glesatinib at 37°C for 3 min. The ATPase reaction was induced by the addition of 5 mM of Mg-ATP, and the total volume was 0.1 mL. After incubation

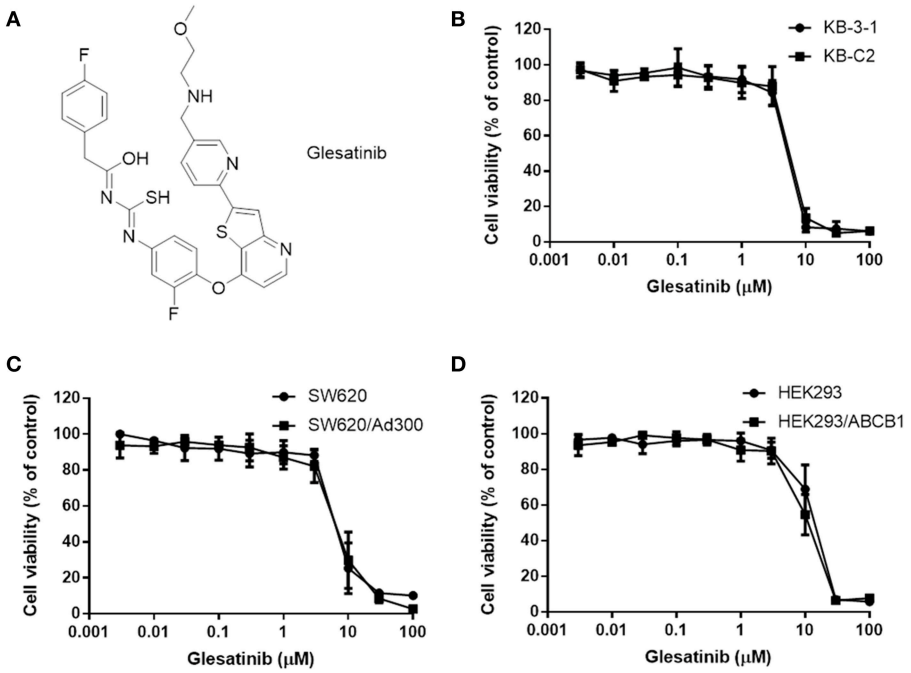

FIGURE 1 | The structure of glesatinib and its cytotoxic effects to three P-gp overexpressing cancer cells. **(A)** Chemical structure of glesatinib. **(B)** Concentration -dependent viability curves for KB-3-1 and KB-C2 cell lines incubated with different concentration of glesatinib for 72 h. **(C)** Concentration-dependent viability curves for SW620 and SW620/Ad300 cell lines incubated with different concentration of glesatinib for 72 h. **(D)** Concentration-dependent viability curves for HEK293/pcDNA3.1 and HEK293/ABCB1 cells incubated with different concentration of glesatinib for 72 h. The cell viability was determined by MTT assay. Data are expressed as mean ± SD, and representative of three independent experiments in triplicate are shown.

at 37°C for 20 min, the reaction was allowed to continue for another 20 min at 37°C and then terminated by adding 100 μL of a 5% SDS solution to the reaction mix. The amount of inorganic phosphate (IP) release was detected at 880 nm using a spectrophotometer.

[^{3}H]-Paclitaxel Accumulation and Efflux Assay

Since glesatinib reversed MDR mediated by P-gp, the reversal mechanism may be related to change of the protein expression or location of P-gp, we used the drug accumulation and efflux assays to determine the reversal mechanism as previously described (27). The accumulation and efflux of [^{3}H]-paclitaxel in KB-3-1 and KB-C2 cells were measured in the absence or presence of glesatinib (1, 3 μM), and verapamil (3 μM) was used as positive control.

Molecular Modeling of Human ABCB1 Homology Model

To reveal more details of the interaction between glesatinib and P-gp, we conducted docking study. All docking experiments were performed following the reported protocols with software Schrodinger 2018–1 (Schrödinger, LLC, New York, NY, 2018) on a Mac Pro 6-core Intel Xenon X5 processor with Macintosh Operating System (OS X El Capitan) (28, 37). Ligand preparation was essentially performed. Human P-gp homology model (4M1M) was established by Dr. S. Aller based on improved mouse P-gp (3G5U). Single-wavelength anomalous diffraction (SAD) phasing was conducted to the full 3.8 Å resolution of the dataset. Non-crystallographic symmetry (NCS) operators were determined from the mouse P-gp structure with the phenix.python script simple_ncs_from_pdb.py. Refinement was conducted with phenix.refine using NCS and secondary structure restraints, restraining NCS-related B-factors, group B-factor and individual B-factor (38). The centroid of some important residues including H61, G64, L65, M68, L339, A342, L975 C343, F942, T945, Q946, Y950, L975, V982, and A985 (39–41). Glide XP docking was performed and the receptor grid for induced-fit docking (IFD) was generated by selecting residues. Then IFD was conducted with the default protocol.

Statistical Analysis

All data are expressed as the mean ± SD. All experiments were repeated at least three times and the data were analyzed using a one-way or two-way ANOVA by GraphPad Prism 7.00 software. Differences were considered significant when $P < 0.05$.

RESULTS

Glesatinib Antagonized MDR in P-gp Overexpressing Cancer Cells

First, the cytotoxicity of glesatinib to P-gp overexpressing cancer cells KB-C2, SW620/Ad300, HEK293/ABCB1, and their parent cells KB-3-1, SW620, HEK293 cells were determined by MTT

assay. As shown in **Figures 1B–D**, the IC_{50}s fell between 5 and 10 μM. Therefore, the non-toxic concentration (IC_{20}) of glesatinib applied in the reversal effects evaluation were 1 and 3 μM.

The reversal effects of glesatinib to P-gp substrates, including doxorubicin, paclitaxel and colchicine were further tested in the aforementioned cancer cells. The non-selective P-gp inhibitor, verapamil was used as a positive control (42), and non-substrate cisplatin was used as a negative control (43). Pretreatment with or without glesatinib with these substrates to P-gp overexpressing cancer cells and their sensitive parent cells were tested to obtain their IC_{50}s.

As shown in **Tables 1**, **2**, the parent cells were sensitive to doxorubicin, paclitaxel and colchicine, and the IC_{50}s were as low as nano-mole. While P-gp overexpressing cancer cell exhibited resistant properties to these chemotherapeutics, resistance fold ranged from 77 to 438. Pretreatment with glesatinib significantly lowered the IC_{50}s of all these three chemotherapeutics to resistant cancer cells. More importantly, glesatinib exhibited similar re-sensitizing effects to P-gp transfected HEK293/ABCB1 cells, suggesting its mechanisms of re-sensitizing to chemotherapeutics were directly or indirectly related to P-gp. In addition, in ABCG2 overexpressing cancer cells NCI-H460/MX20 cells, gleasatinib failed to reverse topotecan (an ABCG substrate) resistance (**Table 2**). These results indicated that glesatinib could antagonize cancer MDR mediated by P-gp, but not MDR mediated by ABCG2.

Glesatinib Did Not Impact the P-gp Expression and Subcellular Localization

The down-regulation or re-localization of P-gp (from cellular membrane to cytosol) may lead to re-sensitization of chemotherapeutics as a result of less extent of efflux or unable to exert its functions (17, 44). We further determined the interaction mechanism of glesatinib with P-gp by examining the P-gp expression and cellular location through Western blotting and immunofluorescence assay. P-gp overexpressing KB-C2 cells were treated with glesatinib at different concentration (0.3, 1, 3 μM for 72 h) or at different time (3 μM for 24, 48, 72 h) and the P-gp expression was examined. SW620/Ad300 cells were treated with 3 μM for 0, 24, 48, 72 h to examine the localization of P-gp. KB-3-1 and SW620 cells were used as negative control in this experiment.

As shown in **Figure 2**, P-gp expression was not impacted by glesatinib either dose- or time-dependently. The immunofluorescence assay results of **Figure 3** showed that after treatment of glesatinib, localization of P-gp had not changed and remained to localize on the cell membrane. These results suggested that glesatinib could not impact the expression and localization of P-gp. We next tested the effects of glesatinib to the efflux functions of P-gp.

Glesatinib Increased the Intracellular [^{3}H]-Paclitaxel Accumulation and Inhibited [^{3}H]-Paclitaxel Efflux in Cancer Cell Lines Overexpressing P-gp

As glesatinib did not alter either P-gp expression or its localization, we set out to test the transporting function of P-gp by examining the cellular accumulation of radioactive [^{3}H]-paclitaxel. As shown in **Figures 4A,B**, in KB-3-1 cells that barely expressed P-gp, [^{3}H]-paclitaxel had not been impacted, and glesatibin had no effects to either the drug accumulation (**Figure 4A**) or efflux (**Figure 4B**).

TABLE 1 | Glesatinib sensitized paclitaxel, colchicine, and doxorubicin to P-gp-overexpressing cell lines (KB-C2 and HEK293/ABCB1 cells).

Treatment	IC_{50} ± SD[a] (RF[b])			
	KB-3-1 (μM)	KB-C2 (μM)	HEK293 (μM)	HEK293/ABCB1 (μM)
Paclitaxel	0.004 ± 0.002 (1.00)	1.755 ± 0.057 (438.75)	0.073 ± 0.027 (1.00)	3.757 ± 0.312 (51.46)
+ Gle (1 μM)	0.004 ± 0.001 (1.00)	0.220 ± 0.026 (55)*	0.122 ± 0.050 (1.67)	0.255 ± 0.084 (3.49)*
+ Gle (3 μM)	0.003 ± 0.001 (0.75)	0.015 ± 0.001 (3.75)*	0.100 ± 0.020 (1.37)	0.047 ± 0.004 (0.64)*
+ Vera (3 μM)	0.003 ± 0.001 (0.75)	0.010 ± 0.002 (2.5)*	0.068 ± 0.003 (0.95)	0.094 ± 0.003 (1.9)*
Doxorubicin	0.032 ± 0.013 (1.00)	2.504 ± 0.487 (78.25)	0.061 ± 0.020 (1.00)	0.631 ± 0.150 (10.34)
+ Gle (1 μM)	0.029 ± 0.003 (0.91)	0.118 ± 0.061 (3.69)*	0.060 ± 0.029 (0.98)	0.072 ± 0.006 (1.18)*
+ Gle (3 μM)	0.028 ± 0.004 (0.88)	0.023 ± 0.010 (0.72)*	0.066 ± 0.009 (1.08)	0.064 ± 0.021 (1.05)*
+ Vera (3 μM)	0.024 ± 0.006 (0.75)	0.024 ± 0.005 (0.75)*	0.061 ± 0.008 (1.00)	0.084 ± 0.009 (1.38)*
Colchicine	0.009 ± 0.002 (1.00)	3.231 ± 0.260 (359.00)	0.066 ± 0.001 (1.00)	1.538 ± 0.090 (23.30)
+ Gle (1 μM)	0.006 ± 0.002 (0.67)	0.993 ± 0.183 (110.33)*	0.058 ± 0.007 (0.88)	0.126 ± 0.106 (1.91)*
+ Gle (3 μM)	0.007 ± 0.001 (0.78)	0.088 ± 0.020 (9.78)*	0.048 ± 0.009 (0.73)	0.047 ± 0.021 (0.71)*
+ Vera (3 μM)	0.009 ± 0.001 (1.00)	0.116 ± 0.035 (12.89)*	0.056 ± 0.006 (0.85)	0.050 ± 0.008 (0.76)*
Cisplatin	2.508 ± 0.432 (1.00)	3.027 ± 0.343 (1.21)	2.660 ± 0.430 (1.00)	3.336 ± 0.451 (1.25)
+ Gle (1 μM)	1.990 ± 0.452 (0.79)	2.676 ± 0.443 (1.07)	1.982 ± 0.253 (0.75)	3.272 ± 0.254 (1.23)
+ Gle (3 μM)	2.031 ± 0.364 (0.81)	2.120 ± 0.152 (0.85)	1.903 ± 0.361 (0.72)	3.394 ± 0.353 (1.28)
+ Vera (3 μM)	2.309 ± 0.641 (0.92)	2.098 ± 0.230 (0.84)	2.388 ± 0.452 (0.90)	3.115 ± 0.433 (1.17)

*$P < 0.05$ vs. no inhibitor group.

[a] IC_{50} values represented the mean ± SD of three independent experiments performed in triplicate.

[b] Resistance fold (RF) was calculated by dividing the IC50 values of substrates in the presence or absence of an inhibitor by the IC_{50} values of parental cells without an inhibitor. Gle, Glesatinib; Vera, verapamil.

TABLE 2 | Glesatinib sensitized paclitaxel, colchicine, and doxorubicin to P-gp-overexpressing cell line (SW620/Ad300 cells), but not topotecan to ABCG2-overexpressing cells (NCI-H460/MX20 cells).

Treatment	IC_{50} ± SD[a] (RF[b])		Treatment	IC_{50} ± SD[a] (RF[b])	
	SW620 (μM)	SW620/Ad300 (μM)		NCI-H460 (μM)	NCI-H460/MX20 (μM)
Paclitaxel	0.091 ± 0.015 (1.00)	21.190 ± 6.25 (232.86)	Topotecan	0.063 ± 0.020 (1.00)	6.010 ± 0.530 (95.49)
+ Gle (1 μM)	0.067 ± 0.013 (0.74)	1.969 ± 0.160 (21.63)*	+ Gle (1 μM)	0.060 ± 0.015 (0.95)	6.360 ± 0.127 (100.95)
+ Gle (3 μM)	0.060 ± 0.020 (0.66)	0.257 ± 0.072 (2.82)*	+ Gle (3 μM)	0.040 ± 0.021 (0.63)	7.160 ± 1.193 (113.65)
+ Vera (3 μM)	0.097 ± 0.031 (1.07)	0.646 ± 0.173 (7.10)*	+ Ko 143 (3 μM)	0.051 ± 0.013 (0.81)	0.520 ± 0.130 (8.25)*
Doxorubicin	0.031 ± 0.014 (1.00)	9.950 ± 2.023 (320.97)	Cisplatin	1.640 ± 0.185 (1.00)	2.150 ± 0.498 (1.31)
+ Gle (1 μM)	0.033 ± 0.007 (1.06)	2.397 ± 0.041 (77.32)*	+ Gle (1 μM)	1.699 ± 0.392 (1.04)	1.926 ± 0.297 (1.17)
+ Gle (3 μM)	0.029 ± 0.012 (0.94)	0.271 ± 0.020 (8.74)*	+ Gle (3 μM)	1.513 ± 0.218 (0.92)	2.049 ± 0.187 (1.25)
+ Vera (3 μM)	0.023 ± 0.007 (0.74)	0.288 ± 0.155 (9.29)*	+ Ko 143 (3 μM)	1.686 ± 0.152 (1.03)	2.285 ± 0.138 (1.39)
Cisplatin	1.481 ± 0.676 (1.00)	1.514 ± 0.398 (1.02)			
+ Gle (1 μM)	1.266 ± 0.189 (0.85)	1.676 ± 0.138 (1.13)			
+ Gle (3 μM)	1.166 ± 0.079 (0.79)	1.587 ± 0.329 (1.07)			
+ Vera (3 μM)	1.164 ± 0.107 (0.79)	1.851 ± 0.364 (1.25)			

*$P < 0.05$ vs. no inhibitor group.

[a] IC_{50} values represented the mean ± SD of three independent experiments performed in triplicate.

[b] Resistance fold (RF) was calculated by dividing the IC_{50} values of substrates in the presence or absence of an inhibitor by the IC_{50} values of parental cells without an inhibitor. Gle, Glesatinib; Vera, verapamil.

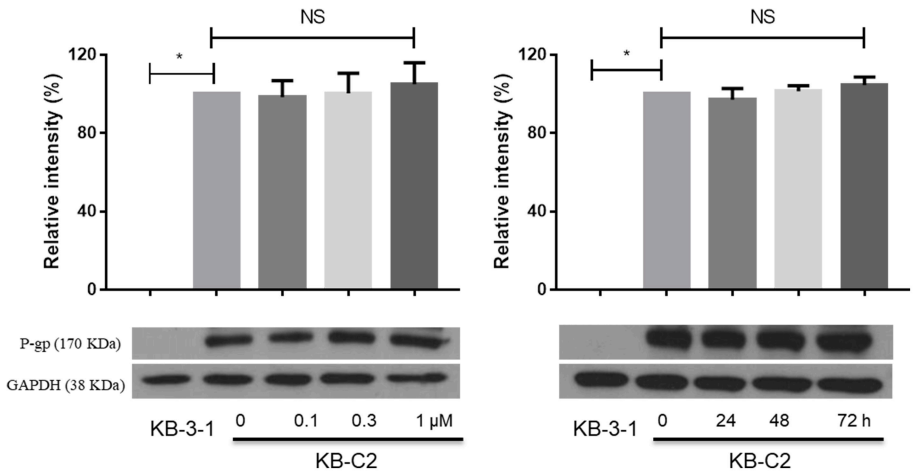

FIGURE 2 | Glesatinib did not affect the protein expression of P-gp transporters in ABCB1 overexpressing cell lines. Detection and relative intensity of ABCB1 expression in KB-C2 cells incubated with 0.3, 1, 3 μM for 72 h and 3 μM for 0, 24, 48, 72 h. Data are mean ± SD, representative of three independent experiments. *$p < 0.05$, compared with control group.

While in P-gp overexpressing KB-C-2 cells, [^{3}H]-paclitaxel accumulation decreased significantly as shown in **Figures 4A,C**. Pretreatment of glesatinib may significantly increase the [^{3}H]-paclitaxel accumulation and inhibited the drug efflux of P-gp. These results indicated that glesatinib may exert its re-sensitizing effects by thwart the transporting function of P-gp.

Glesatinib Stimulated the ATPase Activity of P-gp

ATP hydrolyzed by ATPase was used by P-gp to provide the energy to transport its substrates (45, 46). To further reveal the P-gp inhibitory mechanisms, we determined the effect of glesatinib on the ATPase activity of P-gp transporters by measuring P-gp-mediated ATP hydrolysis in the presence or absence of glesatinib (0–40 μM). As shown in **Figure 5**, Glesatinib stimulated the ATPase activity of P-gp transporters in a dose-dependent manner. The concentration of 50% stimulation was 3.2 μM, and the maximum stimulation was 5.59-fold greater than that of basal level.

Induced-Fit Docking (IFD) Simulation Interactions Between P-gp and Glesatinib

We investigated the potential interaction of glesatinib with P-gp by conducting docking analysis. The best docking score of the binding of glesatinib and human P-gp was −12.639 kcal/mol. The best-scored docked position of glesatinib with P-gp was showed

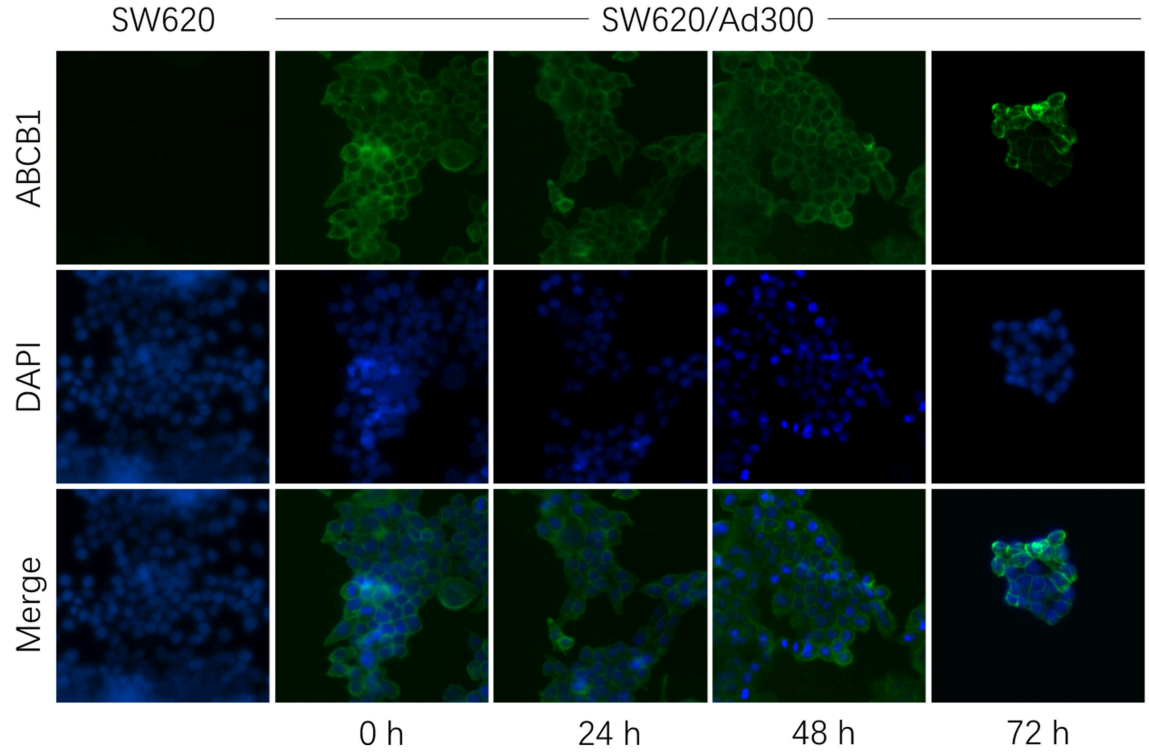

FIGURE 3 | Glesatinib did not affect the localization of ABCB1 transporters in ABCB1 overexpressing cell lines. Sub-cellular localization of ABCB1 expression in SW620/Ad300 cells incubated with 3 μM of glesatinib for 0, 24, 48, and 72 h. ABCB1, green and DAPI (blue) counterstains the nuclei. SW620 cells represented the control group.

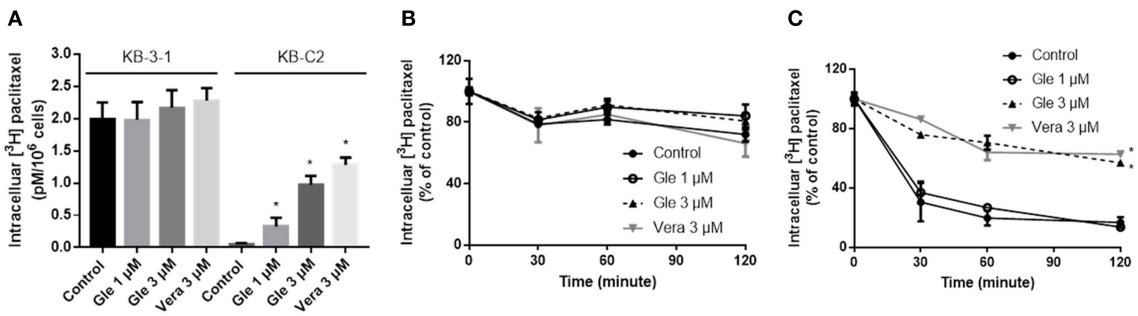

FIGURE 4 | Glesatinib increased the accumulation and inhibited the efflux of [^{3}H]-paclitaxel in P-gp overexpressing KB-C2 cells. **(A)** The effect of glesatinib on the accumulation of [^{3}H]-paclitaxel in KB-3-1 and KB-C2 cell lines. **(B)** The effect of glesatinib on efflux of [^{3}H]-paclitaxel in KB-3-1 and **(C)** KB-C2. Verapamil (3 μM) was used as positive controls. Data are mean ± SD, representative of three independent experiments. *$p < 0.05$, compared with control group. Gle, Glesatinib; Vera, verapamil.

in **Figure 6**. There were two hydrogen bonds between glesatinib and human P-gp, including the hydrogen binding between the amide group of glesatinib and Tyr950 (C=O…HO-Tyr950), in addition with the hydrogen bond between the methoxy group and Asn721 (H_3C-O…H_2N-Asn721). The fluorophenyl group of glesatinib has π-π interaction with both Phe336 and Phe983 of P-gp protein. The thienopyridine group has π-π interaction with the residues Phe728 and Phe983. Interestingly, the acidic microenvironment of tumor (47) could result in the ionization of glesatinib, and the amine cation could form a hydrogen bond with Tyr307 and a π-cation bond with Phe303. These formed various bonds between glesatinib and human P-gp may finally lead to the collapsed P-gp.

DISCUSSION

ABC transporter P-gp functions as the protective enzyme that pumps out xenobiotics including many chemotherapeutics that are its substrates, causing MDR in cancers (3). To counter that, many P-gp inhibitors have been developed and some of them have been tested in clinical trials, while all of them have failed to get approved by US

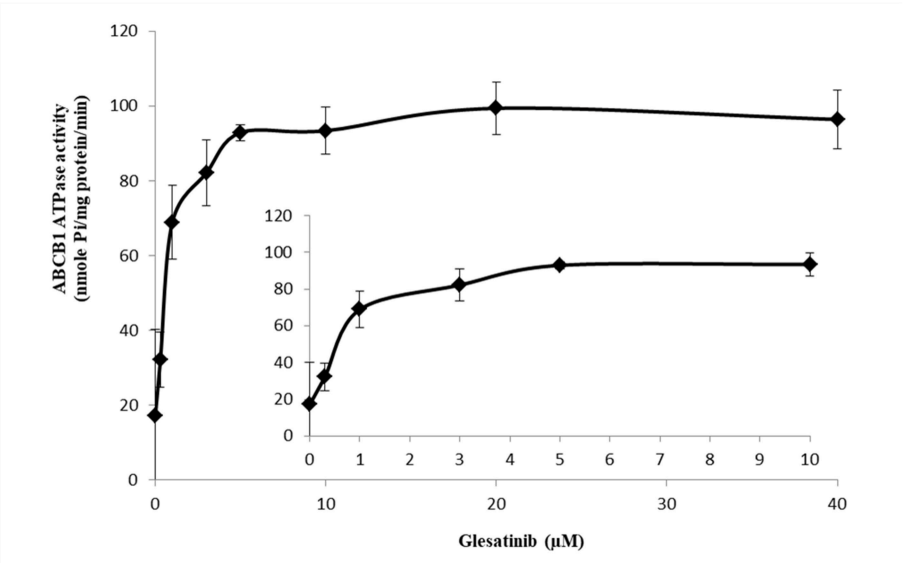

FIGURE 5 | Glesatinib stimulated the ATPase activity of P-gp. Effect of various concentrations of glesatinib on the ATPase activity of P-gp. The inset graphs illustrate the effect of 0–10 μM glesatinib on the ATPase activity of P-gp. Data are mean ± SD, representative of three independent experiments.

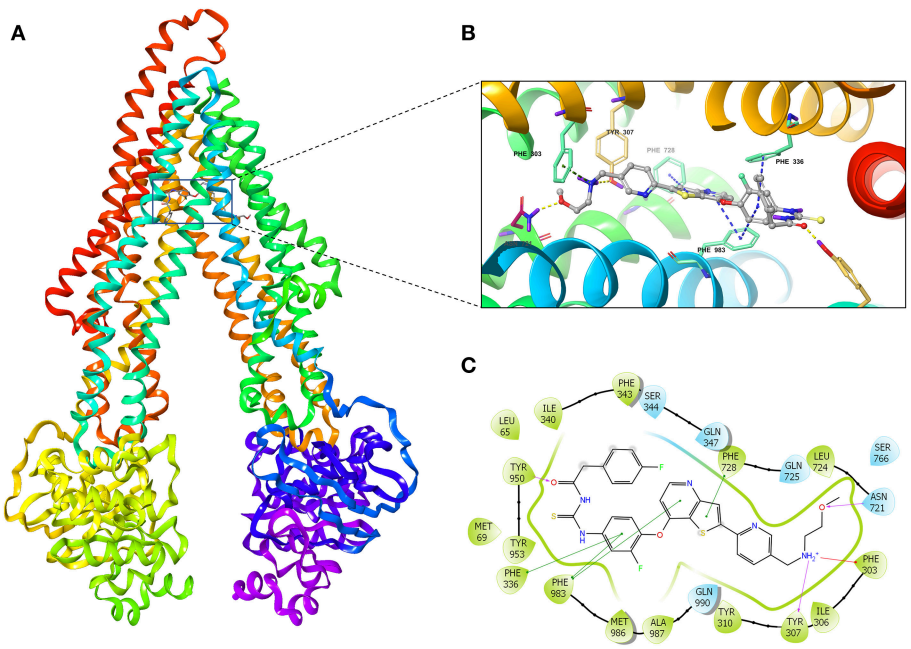

FIGURE 6 | The molecular modeling study of glesatinib with human homology ABCB1. **(A)** Overall view of glesatinib-P-gp complex. **(B)** 3D figure of Docked position of glesatinib within the drug-binding site of human P-gp homology model. Glesatinib was showed as ball and stick mode with the atoms colored: carbon-cyan, nitrogen-blue, oxygen-red, fluorine-green, sulfur-yellow, hydrogen-purple. Important residues were showed as sticks, with the color pattern: carbon-gray, nitrogen-blue, oxygen-red, hydrogen-purple. π-π stacking interactions are indicated with cyan dotted line. π-cation bond is indicated with green dotted line. Hydrogen bonds were showed by the yellow dotted line. **(C)** 2D figure of Docked position of glesatinib within the drug-binding site of human P-gp homology model. The cyan bubbles indicate polar residues and the green bubbles indicate hydrophobic residues. Hydrogen bonds are shown by the purple dotted arrow. π-π stacking interactions are shown by the green lines and π-cation bond is indicated with red line.

FDA due to severely adverse effects (48, 49). Recent studies indicate that certain TKIs may work as regulators of P-gp (2, 50), either inhibiting its expression (51) or impact its functions (35). Combinations of these TKIs and chemotherapeutics hold promising potential in the treatment of MDR cancers.

In this work, we found that MET/SMO dual inhibitor glesatinib, a drug candidate that is now under clinical trials, antagonized P-gp mediated MDR in cancer cells overexpressing P-gp. As shown in SW620/Ad300 and KB-C2 cells, glesatinib could antagonized P-gp mediated resistance by significantly reducing the IC_{50}s of doxorubicin, paclitaxel and colchicine, while had no effects to cisplatin which was not a substrate of P-gp. To confirm these effects were mediated by P-gp, we further tested its reversal effects to P-gp transpected HEK293 cells. Glesatinib exhibited similar effects in HEK293/ABCB1 cells, indicating the effects were mediated by regulating P-gp. We further confirmed that glesatinib did not affect the expression and sub-cellular localization of P-gp, while it could stimulate ATPase, similar as P-gp inhibitor verapamil (45). Importantly, our results showed gleastinib significantly increased the intracellular accumulation of [^{3}H]-paclitaxel and suppressed the efflux effects, which may contribute to the increased cytotoxic effects when used by combination. Finally, the docking study indicated that glesatinib might have strong interaction with P-gp via hydrogen bonds and π-π interaction, leading to the efflux inhibition. This docking result may provide valuable information to develop glesatinib derivatives for better targeting and/or binding.

In conclusion, MET/SMO dual inhibitor Glesatinib antagonized P-gp mediated MDR by inhibiting its efflux functions. This work provided important information for further clinical trials.

AUTHOR CONTRIBUTIONS

QC and Z-SC: conception and design. QC, C-YC, H-LG, NJ, SS, SA, and Z-SC: development of methodology. QC, C-YC, H-LG, PG, and NJ: acquisition of data. QC, C-YC, H-LG, NJ, and Z-SC: analysis and interpretation of data. QC, C-YC, LR, YY, D-HY, and Z-SC: writing, review, and/or revision of the manuscript. All authors read and approved the final manuscript.

ACKNOWLEDGMENTS

We thank Dr. Stephen Aller for providing the human ABCB1 homology model. We thank Dr. Tanaji T. Talele for providing the computing resources for the docking study. We thank Drs. Susan E. Bates and Robert W. Robey (NCI, NIH, Bethesda, MD) for providing the cell lines. We thank the support of Guangzhou Postdoctoral Foundation of International Training for QC and NIH funding (No. 1R15GM116043-01) to Z-SC.

REFERENCES

1. Housman G, Byler S, Heerboth S, Lapinska K, Longacre M, Snyder N, et al. Drug resistance in cancer: an overview. *Cancers*. (2014) 6:1769–92. doi: 10.3390/cancers6031769
2. Shukla S, Chen ZS, Ambudkar SV. Tyrosine kinase inhibitors as modulators of ABC transporter-mediated drug resistance. *Drug Resist Updat.* (2012) 15:70–80. doi: 10.1016/j.drup.2012.01.005
3. Robey RW, Pluchino KM, Hall MD, Fojo AT, Bates SE, Gottesman MM. Revisiting the role of ABC transporters in multidrug-resistant cancer. *Nat Rev Cancer*. (2018) 18:452–64. doi: 10.1038/s41568-018-0005-8
4. Kathawala RJ, Gupta P, Ashby CJ, Chen ZS. The modulation of ABC transporter-mediated multidrug resistance in cancer: a review of the past decade. *Drug Resist Updat.* (2015) 18:1-17. doi: 10.1016/j.drup.2014.11.002
5. Xue M, Cheng J, Zhao J, Zhang S, Jian J, Qiao Y, et al. Outcomes of 219 chronic myeloid leukaemia patients with additional chromosomal abnormalities and/or tyrosine kinase domain mutations. *Int J Lab Hematol.* (2018) 41:94–101. doi: 10.1111/ijlh.12928
6. Taylor S, Spugnini EP, Assaraf YG, Azzarito T, Rauch C, Fais S. Microenvironment acidity as a major determinant of tumor chemoresistance: proton pump inhibitors (PPIs) as a novel therapeutic approach. *Drug Resist Updat.* (2015) 23:69–78. doi: 10.1016/j.drup.2015.08.004
7. Cui Q, Wen S, Huang P. Targeting cancer cell mitochondria as a therapeutic approach: recent updates. *Future Med Chem.* (2017) 9:929–49. doi: 10.4155/fmc-2017-0011
8. Rashmi R, Huang X, Floberg JM, Elhammali AE, McCormick ML, Patti GJ, et al. Radioresistant cervical cancers are sensitive to inhibition of glycolysis and redox metabolism. *Cancer Res.* (2018) 78:1392–403. doi: 10.1158/0008-5472.CAN-17-2367
9. Centurione L, Aiello FB. DNA repair and cytokines: TGF-beta, IL-6, and thrombopoietin as different biomarkers of radioresistance. *Front Oncol.* (2016) 6:175. doi: 10.3389/fonc.2016.00175
10. Yoshimoto K, Mizoguchi M, Hata N, Murata H, Hatae R, Amano T, et al. Complex DNA repair pathways as possible therapeutic targets to overcome temozolomide resistance in glioblastoma. *Front Oncol.* (2012) 2:186. doi: 10.3389/fonc.2012.00186
11. Bekaii-Saab T, El-Rayes B. Identifying and targeting cancer stem cells in the treatment of gastric cancer. *Cancer Am Cancer Soc.* (2017) 123:1303–12. doi: 10.1002/cncr.30538
12. Prieto-Vila M, Takahashi RU, Usuba W, Kohama I, Ochiya T. Drug resistance driven by cancer stem cells and their niche. *Int J Mol Sci.* (2017) 18:E2574. doi: 10.3390/ijms18122574
13. Cui Q, Wang JQ, Assaraf YG, Ren L, Gupta P, Wei L, et al. Modulating ROS to overcome multidrug resistance in cancer. *Drug Resist Updat.* (2018) 41:1–25. doi: 10.1016/j.drup.2018.11.001
14. Zhang G, Wang W, Yao C, Ren J, Zhang S, Han M. Salinomycin overcomes radioresistance in nasopharyngeal carcinoma cells by inhibiting Nrf2 level and promoting ROS generation. *Biomed Pharmacother.* (2017) 91:147–54. doi: 10.1016/j.biopha.2017.04.095
15. Ceballos MP, Rigalli JP, Cere LI, Semeniuk M, Catania VA, Ruiz ML. ABC transporters: regulation and association with multidrug resistance in hepatocellular carcinoma and colorectal carcinoma. *Curr Med Chem.* (2018) doi: 10.2174/0929867325666180105103637. [Epub ahead of print].
16. Chen ZS. ABC transporters in pharmacology/physiology and human diseases. *Curr Pharm Biotechnol.* (2011) 12:569. doi: 10.2174/138920111795163940
17. Fu D. Where is it and how does it get there—intracellular localization and traffic of P-glycoprotein. *Front Oncol.* (2013) 3:321. doi: 10.3389/fonc.2013.00321
18. Zinzi L, Capparelli E, Cantore M, Contino M, Leopoldo M, Colabufo NA. Small and innovative molecules as new strategy to revert MDR. *Front Oncol.* (2014) 4:2. doi: 10.3389/fonc.2014.00002
19. Ezrahi S, Aserin A, Garti N. Basic principles of drug delivery systems—the case of paclitaxel. *Adv Colloid Interface Sci.* (2019) 263:95–130. doi: 10.1016/j.cis.2018.11.004
20. Meyers MB, Scotto KW, Sirotnak FM. P-glycoprotein content and mediation of vincristine efflux: correlation with the level of differentiation in luminal epithelium of mouse small intestine. *Cancer Commun.* (1991) 3:159–65. doi: 10.3727/095535491820873335
21. Bao L, Hazari S, Mehra S, Kaushal D, Moroz K, Dash S. Increased expression of P-glycoprotein and doxorubicin chemoresistance of metastatic breast cancer is regulated by miR-298. *Am J Pathol.* (2012) 180:2490–503. doi: 10.1016/j.ajpath.2012.02.024

22. Frezard F, Pereira-Maia E, Quidu P, Priebe W, Garnier-Suillerot A. P-glycoprotein preferentially effluxes anthracyclines containing free basic versus charged amine. *Eur J Biochem.* (2001) 268:1561–7. doi: 10.1046/j.1432-1327.2001.01989.x
23. Arora A, Shukla Y. Modulation of vinca-alkaloid induced P-glycoprotein expression by indole-3-carbinol. *Cancer Lett.* (2003) 189:167–73. doi: 10.1016/S0304-3835(02)00550-5
24. Leu BL, Huang JD. Inhibition of intestinal P-glycoprotein and effects on etoposide absorption. *Cancer Chemother Pharmacol.* (1995) 35:432–6. doi: 10.1007/s002800050258
25. Palmeira A, Sousa E, Vasconcelos MH, Pinto MM. Three decades of P-gp inhibitors: skimming through several generations and scaffolds. *Curr Med Chem.* (2012) 19:1946–2025. doi: 10.2174/092986712800167392
26. Crowley E, McDevitt CA, Callaghan R. Generating inhibitors of P-glycoprotein: where to, now? *Methods Mol Biol.* (2010) 596:405–32. doi: 10.1007/978-1-60761-416-6_18
27. Ji N, Yang Y, Cai CY, Lei ZN, Wang JQ, Gupta P, et al. Selonsertib (GS-4997), an ASK1 inhibitor, antagonizes multidrug resistance in ABCB1- and ABCG2-overexpressing cancer cells. *Cancer Lett.* (2019) 440–441:82–93. doi: 10.1016/j.canlet.2018.10.007
28. Fan YF, Zhang W, Zeng L, Lei ZN, Cai CY, Gupta P, et al. Dacomitinib antagonizes multidrug resistance (MDR) in cancer cells by inhibiting the efflux activity of ABCB1 and ABCG2 transporters. *Cancer Lett.* (2018) 421:186–98. doi: 10.1016/j.canlet.2018.01.021
29. Gupta P, Zhang YK, Zhang XY, Wang YJ, Lu KW, Hall T, et al. Voruciclib, a potent CDK4/6 inhibitor, antagonizes ABCB1 and ABCG2-mediated multi-drug resistance in cancer cells. *Cell Physiol Biochem.* (2018) 45:1515–28. doi: 10.1159/000487578
30. Zhang YK, Zhang XY, Zhang GN, Wang YJ, Xu H, Zhang D, et al. Selective reversal of BCRP-mediated MDR by VEGFR-2 inhibitor ZM323881. *Biochem Pharmacol.* (2017) 132:29–37. doi: 10.1016/j.bcp.2017.02.019
31. Yang L, Li M, Wang F, Zhen C, Luo M, Fang X, et al. Ceritinib enhances the efficacy of substrate chemotherapeutic agent in human ABCB1-overexpressing leukemia cells *in vitro*, *in vivo* and *ex-vivo*. *Cell Physiol Biochem*. (2018) 46:2487–99. doi: 10.1159/000489655
32. Engstrom LD, Aranda R, Lee M, Tovar EA, Essenburg CJ, Madaj Z, et al. Glesatinib exhibits antitumor activity in lung cancer models and patients harboring MET Exon 14 mutations and overcomes mutation-mediated resistance to type I MET inhibitors in nonclinical models. *Clin Cancer Res.* (2017) 23:6661–72. doi: 10.1158/1078-0432.CCR-17-1192
33. Reungwetwattana T, Liang Y, Zhu V, Ou SI. The race to target MET exon 14 skipping alterations in non-small cell lung cancer: the why, the how, the who, the unknown, and the inevitable. *Lung Cancer.* (2017) 103:27–37. doi: 10.1016/j.lungcan.2016.11.011
34. Shi Z, Tiwari AK, Shukla S, Robey RW, Singh S, Kim IW, et al. Sildenafil reverses ABCB1- and ABCG2-mediated chemotherapeutic drug resistance. *Cancer Res.* (2011) 71:3029–41. doi: 10.1158/0008-5472.CAN-10-3820
35. Ji N, Yang Y, Lei ZN, Cai CY, Wang JQ, Gupta P, et al. Ulixertinib (BVD-523) antagonizes ABCB1- and ABCG2-mediated chemotherapeutic drug resistance. *Biochem Pharmacol.* (2018) 158:274–85. doi: 10.1016/j.bcp.2018.10.028
36. Shukla S, Abel B, Chufan EE, Ambudkar SV. Effects of a detergent micelle environment on P-glycoprotein (ABCB1)-ligand interactions. *J Biol Chem.* (2017) 292:7066–76. doi: 10.1074/jbc.M116.771634
37. Zhang YK, Zhang GN, Wang YJ, Patel BA, Talele TT, Yang DH, et al. Bafetinib (INNO-406) reverses multidrug resistance by inhibiting the efflux function of ABCB1 and ABCG2 transporters. *Sci Rep.* (2016) 6:25694. doi: 10.1038/srep25694
38. Li J, Jaimes KF, Aller SG. Refined structures of mouse P-glycoprotein. *Protein Sci.* (2014) 23:34–46. doi: 10.1002/pro.2387
39. Loo TW, Clarke DM. Mapping the binding site of the inhibitor tariquidar that stabilizes the first transmembrane domain of P-glycoprotein. *J Biol Chem.* (2015) 290:29389–401. doi: 10.1074/jbc.M115.695171
40. Loo TW, Bartlett MC, Clarke DM. Methanethiosulfonate derivatives of rhodamine and verapamil activate human P-glycoprotein at different sites. *J Biol Chem.* (2003) 278:50136–41. doi: 10.1074/jbc.M310448200
41. Loo TW, Clarke DM. Identification of residues in the drug-binding site of human P-glycoprotein using a thiol-reactive substrate. *J Biol Chem.* (1997) 272:31945–8. doi: 10.1074/jbc.272.51.31945
42. Bansal T, Mishra G, Jaggi M, Khar RK, Talegaonkar S. Effect of P-glycoprotein inhibitor, verapamil, on oral bioavailability and pharmacokinetics of irinotecan in rats. *Eur J Pharm Sci.* (2009) 36:580–90. doi: 10.1016/j.ejps.2008.12.005
43. Breier A, Gibalova L, Seres M, Barancik M, Sulova Z. New insight into p-glycoprotein as a drug target. *Anticancer Agents Med Chem.* (2013) 13:159–70. doi: 10.2174/187152013804487380
44. Nobili S, Landini I, Mazzei T, Mini E. Overcoming tumor multidrug resistance using drugs able to evade P-glycoprotein or to exploit its expression. *Med Res Rev.* (2012) 32:1220–62. doi: 10.1002/med.20239
45. Sharom FJ, Yu X, Chu JW, Doige CA. Characterization of the ATPase activity of P-glycoprotein from multidrug-resistant Chinese hamster ovary cells. *Biochem J.* (1995) 308 (Pt 2):381–90. doi: 10.1042/bj3080381
46. Hrycyna CA, Ramachandra M, Ambudkar SV, Ko YH, Pedersen PL, Pastan I, et al. Mechanism of action of human P-glycoprotein ATPase activity. Photochemical cleavage during a catalytic transition state using orthovanadate reveals cross-talk between the two ATP sites. *J Biol Chem.* (1998) 273:16631–4. doi: 10.1074/jbc.273.27.16631
47. Kato Y, Ozawa S, Miyamoto C, Maehata Y, Suzuki A, Maeda T, et al. Acidic extracellular microenvironment and cancer. *Cancer Cell Int.* (2013) 13:89. doi: 10.1186/1475-2867-13-89
48. List AF, Kopecky KJ, Willman CL, Head DR, Slovak ML, Douer D, et al. Cyclosporine inhibition of P-glycoprotein in chronic myeloid leukemia blast phase. *Blood.* (2002) 100:1910–2.
49. Chung FS, Santiago JS, Jesus MF, Trinidad CV, See MF. Disrupting P-glycoprotein function in clinical settings: what can we learn from the fundamental aspects of this transporter? *Am J Cancer Res*. (2016) 6:1583–98.
50. Li W, Zhang H, Assaraf YG, Zhao K, Xu X, Xie J, et al. Overcoming ABC transporter-mediated multidrug resistance: molecular mechanisms and novel therapeutic drug strategies. *Drug Resist Updat.* (2016) 27:14–29. doi: 10.1016/j.drup.2016.05.001
51. Zhang GN, Zhang YK, Wang YJ, Gupta P Jr, Ashby CR, Alqahtani S, et al. Epidermal growth factor receptor (EGFR) inhibitor PD153035 reverses ABCG2-mediated multidrug resistance in non-small cell lung cancer: *in vitro* and *in vivo*. *Cancer Lett.* (2018) 424:19–29. doi: 10.1016/j.canlet.2018.02.040

Conflict of Interest Statement: The authors declare that the research was conducted in the absence of any commercial or financial relationships that could be construed as a potential conflict of interest.